ROYAL SOCIETY
OF CHEMISTRY

PAPER

Check for updates

Design, synthesis and anti-cervical cancer activity of aroylpyrrole-based derivatives as potent histone deacetylase 6 inhibitors

Xingjie Wang,[a] Lixuan Du,[b] Yaxin Xue,[c] Yitong Su,[c] Xuetao Yuan,[a] Shuting Yang,[a] Weiyi Su,[c] Wenli Gou,*[c] Xin Chen [iD] *[d] and Lu Zong*[c]

Cancers, such as cervical carcinoma, are one of the most significant diseases affecting human health and histone deacetylases (HDACs) are striking targets in current antitumor drug development. Compared to pan-HDAC inhibitors with potential toxicity, the development of selective HDAC6 inhibitors (sHDAC6is) is a major research focus. In this study, a series of derivatives bearing an aroylpyrrole core were designed and synthesized using a scaffold-hopping strategy. Among these, the best compound 4-benzoyl-1-(4-fluorobenzyl)-*N*-(7-(hydroxyamino)-7-oxoheptyl)-1*H*-pyrrole-2-carboxamide (**10g**) inhibited HDAC6 with an IC_{50} of 3.9 nM and superior selectivity over HDAC1 compared to ACY-1215. *In vitro*, these aroylpyrroles demonstrated promising antiproliferative activities against Hela and SiHa tumor cells. **10g** also showed superior metabolic stability compared to ACY-1215 in a microsomal stability study. In summary, this work highlighted the therapeutic potential of aroylpyrrole-based sHDAC6 inhibitors and provided a valuable lead compound in treating cervical cancer.

1. Introduction

Gene expression is dynamically regulated by the epigenetic mechanisms of histone acetylation and deacetylation, which directly control chromatin structure.[1] Histone acetyl-transferases act as "writers," adding acetyl groups to histone tails to loosen DNA packaging and promote gene activity. Conversely, histone deacetylases (HDACs) function as "erasers" that remove acetyl groups, and make histones less negatively charged, causing DNA to wrap tighter. Dysregulation in these processes is generally associated with cancer development.[2] HDACs are overexpressed in various diseases such as tumors, nervous dysfunction, inflammation and so on.[3–6] Abundant evidence has established HDACs as promising targets and five drugs have been approved.[7–13] The zinc-dependent HDAC family comprises 11 different isotypes including class I (HDAC1/2/3/8), class II (HDAC4/5/6/7/9/10), and class IV (HDAC11).[14] Class II HDACs could be further subdivided into class IIa and class IIb. Class IIa HDACs (HDAC4/5/7/9) possess low catalytic activity

and function primarily as scaffolding proteins, while class IIb members (HDAC6/10) are predominantly localized in the cytoplasm and exhibit distinct enzymatic activity. Different from other isoforms, HDAC6 contains two tandem catalytic domains which deacetylate a host of cytosolic proteins and non-histone substrates such as α- and β-tubulin, heat shock protein, assembled micro-tubules and cortactin.[15,16] In addition, the unique zinc finger domain in HDAC6 protein facilitates its binding to ubiquitin, thereby regulating protein clearance and degradation. Unlike the lethal effects of deleting HDAC1-3, mice with HDAC6-knocked out are viable and grow normally.[17,18] Therefore, the safety profile and low toxicity make HDAC6i attractive in cancer drug development.[15,19]

To date, many synthetic HDAC6is have been reported.[20–23] Generally, their structures consist of three key components: a cap moiety, a linker, and a zinc-binding group (ZBG) (Fig. 1).[24–27] ACY-1215 (**1**), a clinical candidate for multiple myeloma (MM) and lymphoid malignancies, exhibited potent inhibitory activity against HDAC6 (IC_{50} = 4.7 nM).[28] The combination of ACY-1215 and bortezomib demonstrated synergistic anti-MM effects. Similar to ACY-1215, the second-generation inhibitor ACY-241 (**2**) also showed high potency for HDAC6 (IC_{50} = 4 nM), with 13–18~selectivity over HDAC1-3.[29] KA2507 (**3**) was a potent and selective inhibitor of HDAC6 (IC_{50} = 2.5 nM) in clinical with no dose-limiting toxicities.[30] Preclinical models confirmed its dual function of killing tumor cells and modulating tumor immune microenvironment. Although a lot of sHDAC6is have been successfully developed,

[a] Department of General Surgery, The First Affiliated Hospital of Xi'an Jiaotong University, Xi'an, Shaanxi, 710061, P. R. China

[b] Department of Urology, The First Affiliated Hospital of Xi'an Jiaotong University, Xi'an, Shaanxi, 710061, P. R. China

[c] Department of Obstetrics & Gynecology, The First Affiliated Hospital of Xi'an Jiaotong University, Xi'an, Shaanxi, 710061, P. R. China. E-mail: 13572870556@126.com; catherazong@163.com; Fax: +86-029-85323338

[d] Shaanxi Key Labotory of Natural Products & Chemical Biology, College of Chemistry & Pharmacy, Northwest A & F University, Yangling 712100, P. R. China. E-mail: chenxin1888@nwsuaf.edu.cn; Fax: +87-029-87092335
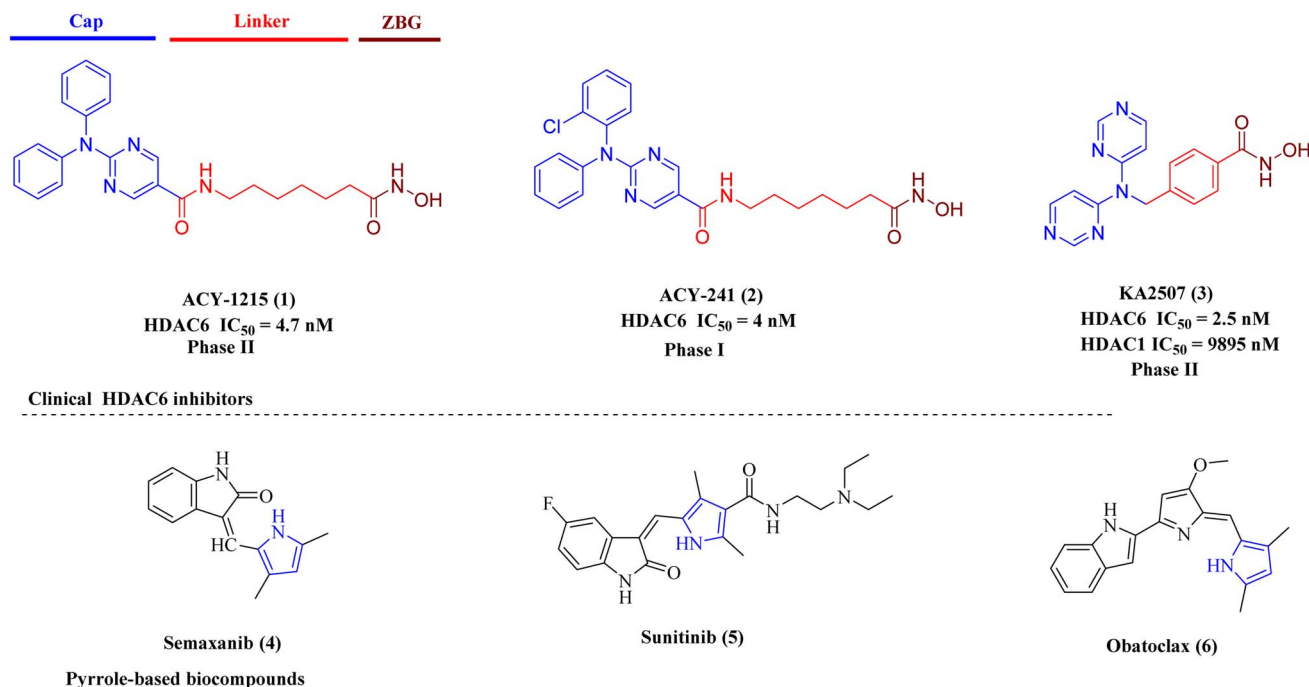
Fig. 1 Clinical selective HDAC6 inhibitors and pyrrole-based biocompounds.

limited efficacy in solid tumors and the risk of toxicity due to insufficient selectivity remains a challenge.[31]

2. Compound design

Structural analysis of ACY-1215, ACY-241, and KA2507 revealed the common pharmacophore: a "Y" shaped capping group, an aliphatic or phenyl linker, and hydroxamic acid as ZBG. In our previous structural derivation of ACY-1215, the cap region demonstrated considerable flexibility for modification.[13] Hence, using drug-like scaffolds as cap moieties is a feasible strategy for HDAC6is design. Pyrrole scaffold was frequently applied in the development of antitumor small molecules (Fig. 1, compounds 4–6).[32–35] In this paper, we designed a new class of HDAC6is by replacing the N, N-diphenylpyrimidine capping group of ACY-1215 with an aroylpyrrole motif, while preserving the six-carbon linker and hydroxamic acid ZBG (Fig. 2). Here, we

reported the synthesis, structure and activity relationship (SAR) study and antiproliferative evaluation of these aroylpyrroles.

3. Chemistry

Given that the N atom of pyrrole was easy to modify and surrounding space was sufficient, we synthesized a series of N-modified analogs to preliminarily probe the SAR. The benzoyl group on 4-position of pyrrole was kept with reference to the structure of ACY-1215. Moreover, the crystal structure of HDAC6 revealed that the cap group located in a large hydrophobic cavity on the surface. Hence, phenyls with various electron-withdrawing or -donating substituents were introduced on pyrrole scaffold. Besides, small aliphatic substituents such as methyl and cyclopropyl were also installed to probe steric tolerance. As shown in Scheme 1, starting material methyl 1H-pyrrole-2-carboxylate (7) reacted with benzoyl chloride yielded key intermediate 8 by Friedel–Crafts reaction. Using sodium
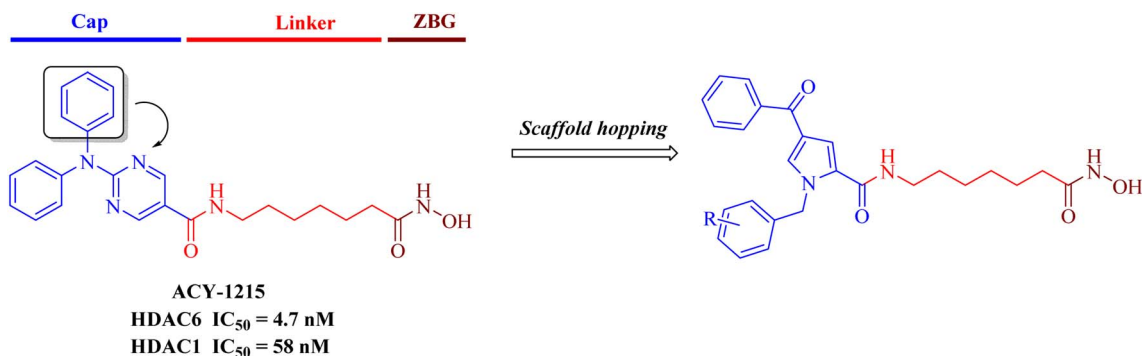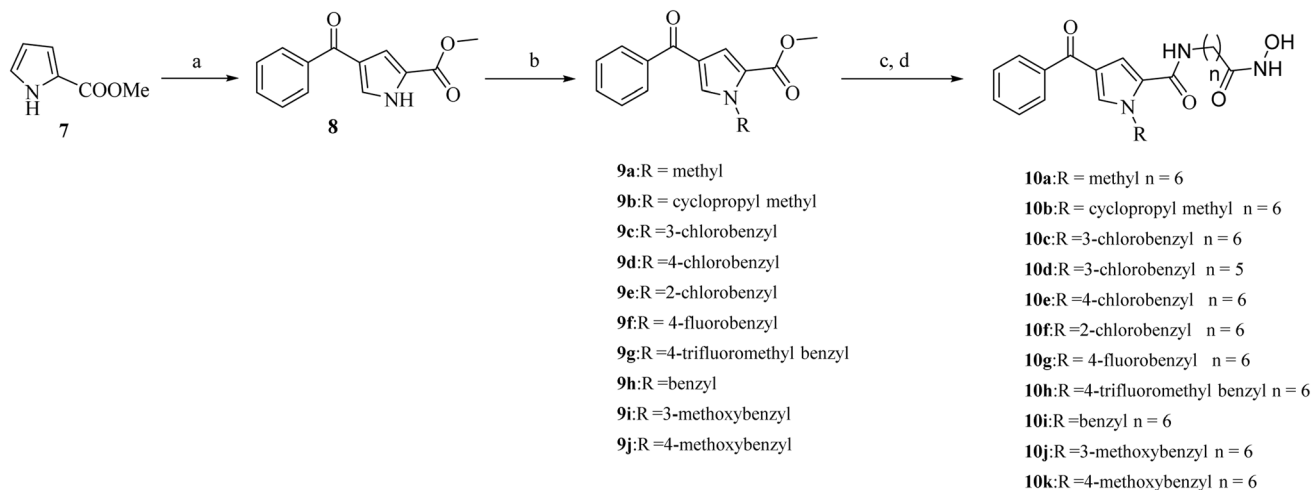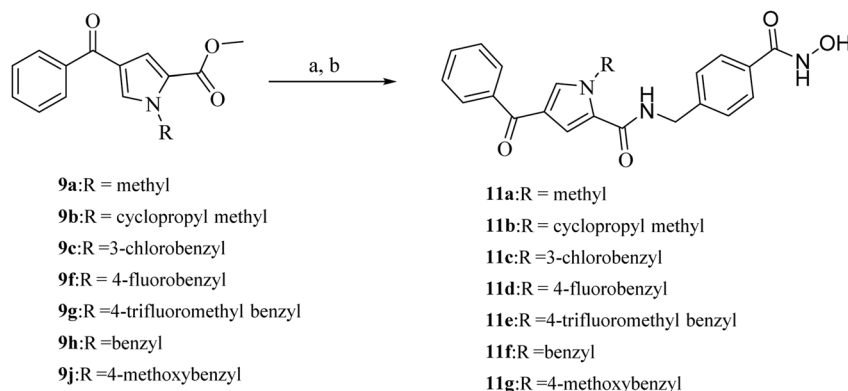

Fig. 2 The design of aroylpyrroles as sHDAC6is.

9a:R = methyl
9b:R = cyclopropyl methyl
9c:R =3-chlorobenzyl
9d:R = 4-chlorobenzyl
9e:R = 2-chlorobenzyl
9f:R = 4-fluorobenzyl
9g:R = 4-trifluoromethyl benzyl
9h:R =benzyl
9i:R = 3-methoxybenzyl
9j:R = 4-methoxybenzyl

10a:R = methyl n = 6
10b:R = cyclopropyl methyl n = 6
10c:R =3-chlorobenzyl n = 6
10d:R =3-chlorobenzyl n = 5
10e:R =4-chlorobenzyl n = 6
10f:R =2-chlorobenzyl n = 6
10g:R = 4-fluorobenzyl n = 6
10h:R =4-trifluoromethyl benzyl n = 6
10i:R =benzyl n = 6
10j:R =3-methoxybenzyl n = 6
10k:R =4-methoxybenzyl n = 6

Scheme 1 Reagents and conditions: (a) PhCOCl, AlCl$_3$, −20 °C to 40 °C, 20 h, 95%; (b) MeI or RCl, NaH, DMF, r.t., 4 h, 68−83%; (c) (i): NaOH, MeOH, 60 °C, 18 h; (ii): HATU, DIPEA, DMF, methyl 7-aminoheptanoate or methyl 6-aminohexanoate, 0 °C, 6 h, 60−75% over 2 steps; (d) NH$_2$OH HCl, KOH, 0 °C to r.t., 4 h, 55−66%.

9a:R = methyl
9b:R = cyclopropyl methyl
9c:R =3-chlorobenzyl
9f:R = 4-fluorobenzyl
9g:R =4-trifluoromethyl benzyl
9h:R =benzyl
9j:R =4-methoxybenzyl

11a:R = methyl
11b:R = cyclopropyl methyl
11c:R =3-chlorobenzyl
11d:R = 4-fluorobenzyl
11e:R =4-trifluoromethyl benzyl
11f:R =benzyl
11g:R =4-methoxybenzyl

Scheme 2 Reagents and conditions: (a) (i): NaOH, MeOH, 60 °C, 18 h; (ii): HATU, DIPEA, DMF, methyl 4-(aminomethyl)benzoate, 0 °C, 6 h, 63−76% over 2 steps; (b) NH$_2$OH HCl, KOH, 0 °C to r.t., 4 h, 51−70%.

hydride as base, the intermediate **9a–j** were obtained through a nucleophilic substitution reaction. Then, condensation of the hydrolysates of **9a–j** with methyl 7-aminoheptanoate or methyl 6-aminohexanoate and following aminolysis by an aqueous NH$_2$OH/KOH solution yielded the target compounds **10a–k**.

To investigate the influence of different linkers on HDAC6 activity, we replaced the aliphatic chain with a phenyl linker. As outlined in Scheme 2, compounds **11a–g** were synthesized with intermediate **9** and methyl 4-(aminomethyl)benzoate following a procedure similar to Scheme 1.
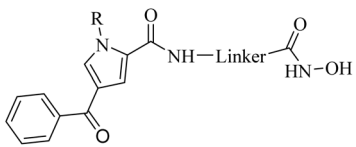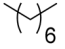
4. Results and discussion
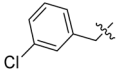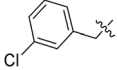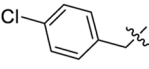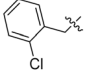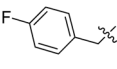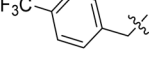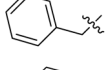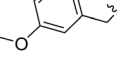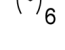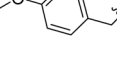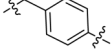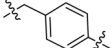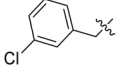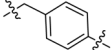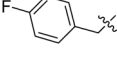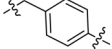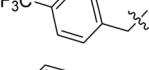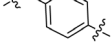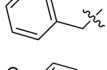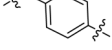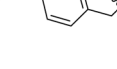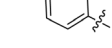
4.1 HDAC1, 6 activities and SAR study of the target compounds

Compounds **10a–k** and **11a–g** were evaluated for HDAC6 inhibitory activity with sHDAC6i ACY1215 and nonselective SAHA as the positive controls. The isoform selectivity was preliminarily assessed against HDAC1. As shown in Table 1, all

eighteen compounds demonstrated nanomolar HDAC6 inhibition. Compounds **10a–c** and **10e–k** with a six-carbon atoms linker showed higher IC$_{50}$ values than those with a five-carbon atoms linker (**10d**) or a rigid benzyl linker (**11a–g**), suggesting the six-carbon chain length was preferred. Among them, the most potent compound **10g** (bearing a *para*-F phenyl), displayed an IC$_{50}$ of 3.9 nM against HDAC6 and a 95-fold selectivity over HDAC1. Other compounds such as **10c**, **10e**, **10f**, **10h–k** also exhibited IC$_{50}$ values ranging from 4.2 nM to 15 nM against HDAC6, with 55–80∼fold selectivity. Substituents on the nitrogen atom of pyrrole core had a significant impact on enzymatic activity and isoform selectivity. The methyl-substituted derivative (**10a**) had an IC$_{50}$ of 20 nM against HDAC6, and it also potently inhibited HDAC1 with IC$_{50}$ of 26.5 nM, while introducing a cyclopropyl group (**10b**) slightly improved inhibition (HDAC6 IC$_{50}$ = 16.5 nM, 2∼fold selectivity). When bulkier hydrophobic phenyl substituents were introduced, both HDAC6 activity and HDAC1 selectivity significantly increased. Specifically, the unsubstituted phenyl

Table 1 Intro inhibitory activities of target compounds **10a–k** and **11a–g** against HDAC1 and HDAC6 (IC_{50}[a], nM)

Compound	R	Linker	HDAC6	HDAC1	Selectivity index
10a	–CH$_3$	⟨6⟩	20.0 ± 1.60	26.5 ± 2.10	1.3
10b	cyclopropyl	⟨6⟩	16.5 ± 1.20	32.1 ± 2.20	2
10c	3-Cl-benzyl	⟨6⟩	12.5 ± 0.80	690 ± 35	60
10d	3-Cl-benzyl	⟨5⟩	68.0 ± 4.50	>10 000	—
10e	4-Cl-benzyl	⟨6⟩	4.20 ± 0.24	790 ± 45	72
10f	2-Cl-benzyl	⟨6⟩	15.0 ± 1.18	825 ± 64	55
10g	4-F-benzyl	⟨6⟩	3.90 ± 0.20	365 ± 23	95
10h	4-F$_3$C-benzyl	⟨6⟩	7.60 ± 0.50	520 ± 46	68
10i	benzyl	⟨6⟩	4.5 ± 0.22	292 ± 18	65
10j	3-OMe-benzyl	⟨6⟩	9.3 ± 0.73	745 ± 55	80
10k	4-OMe-benzyl	⟨6⟩	14.0 ± 0.26	1000 ± 73	71
11a	–CH$_3$	4-benzyl	51.5 ± 3.30	850 ± 68	16.5
11b	cyclopropyl	4-benzyl	78.0 ± 7.50	3120 ± 300	40
11c	3-Cl-benzyl	4-benzyl	94.5 ± 8.30	>10 000	—
11d	4-F-benzyl	4-benzyl	60.0 ± 2.8	>10 000	—
11e	4-F$_3$C-benzyl	4-benzyl	77.0 ± 3.7	>10 000	—
11f	benzyl	4-benzyl	70.0 ± 5.00	>10 000	—
11g	4-OMe-benzyl	4-benzyl	68.0 ± 2.20	>10 000	—
SAHA	—	—	7.40 ± 0.26	4.30 ± 0.15	1.7
ACY1215	—	—	5.13 ± 0.18	62.5 ± 2.30	12

[a] IC_{50} values for enzymatic inhibition of HDAC1 and HDAC6 enzyme. We ran experiments in duplicate, SD < 15%. Assays were performed by Reaction Biology Corporation (Malvern, PA, USA).

Table 2 The screen of **10g** against HDAC isozymes (IC$_{50}$, nM)[b]

| Compound | IC$_{50}$[a] | | | | | | |
	HDAC1	HDAC2	HDAC3	HDAC4	HDAC5	HDAC6	HDAC8
10g	365 ± 22.5	659 ± 43	1150 ± 82	>50 000	>50 000	3.90 ± 0.20	920 ± 50
SAHA	4.30 ± 0.15	11.5 ± 0.25	3.50 ± 0.12	> 50 000	>50 000	7.40 ± 0.26	1030 ± 13
ACY1215	62.5 ± 2.30	47.2 ± 1.76	51.0 ± 3.60	7250 ± 430	5100 ± 270	5.13 ± 0.18	130 ± 9.20

[a] IC$_{50}$ values for enzymatic inhibition of HDAC family. We ran experiments in duplicate, SD < 15%. Assays were performed by Reaction Biology Corporation (Malvern, PA, USA). [b] ND = not determined.

derivative **10i** exhibited an IC$_{50}$ of 4.5 nM and 65-fold selectivity, and introducing *para*-Cl (**10e**), -F (**10g**) or -OMe (**10k**) substituents maintained inhibitory activity and slightly improved selectivity. However, *meta*-Cl, and *ortho*-Cl substitutions (**10c**, **10f**) resulted in a reduction on potency than *para*-substituted counterpart (**10e**) which was also validated by **10j** and **10k**.

Compound **10g** was further tested for isoform selectivity against other HDACs including HDAC2/3/4/5/8. As demonstrated in Table 2, **10g** exhibited weak inhibition against HDAC2, HDAC3, and HDAC8, with IC$_{50}$ values of 659 nM, 1150 nM, and 920 nM, respectively. It had no obvious activity against HDAC4 and HDAC5.

4.2 Molecular simulation

The most potent compound **10g** was docked into the crystal structure of human HDAC6 (PDB code: 5EDU) to elucidate the possible interaction model. As shown in Fig. 3A, the aliphatic chain linker located in the hydrophobic channel formed by Phe620 and Phe680, and enabled the hydroxamic acid group to access the bottom of the binding pocket. The carbonyl and hydroxyl of hydroxamic acid coordinated with Zn^{2+} in a bidentate geometry, with Zn^{2+}–O distances of 2.2 Å (hydroxyl group) and 2.1 Å (carbonyl group) respectively. Additionally, the residues of His610 and Asp649 further stabilized the interaction by forming two hydrogen bonds with hydroxamate. The pyrrole

group served as a suitable fragment in cap region, making the two phenyl substituents match well with the protein surface (Fig. 3B).

4.3 Antiproliferative activities of representative compounds

Cervical cancer is one of the most threatening malignant tumors to women's health worldwide.[36,37] HDACs are important targets in the pathogenesis and metastatic invasion of cervical cancer,[38,39] and cervical cancer cell such as Hela cells was widely used in HDACis research during the past few decades.[40–42] However, there is still limited literatures about the application of sHDAC6is in cervical cancer research. Hence, exploration of HDAC6 inhibitor in cervical cancer treatment is necessary and valuable. Based on the inspiring results in Table 2, compounds **10e** and **10g–i** with better enzymatic activity were selected for antiproliferative evaluation against two cervical cancer cell lines Hela and SiHa, using ACY-1215 and SAHA as the positive compounds. As seen in Table 3, all tested compounds exhibited potent antiproliferative activities with IC$_{50}$ values in single-digit micromolar level. Although less potent than SAHA, their antiproliferative activity was superior to that of ACY1215. **10g** showed the best growth inhibition against Hela and SiHa tumor cells with IC$_{50}$ values of 2.0 and 4.6 μM, respectively. Compound **10i** also exhibited good antiproliferative activity comparable to that of **10g**. Moreover, **10g** and **10i** showed no significant toxicity
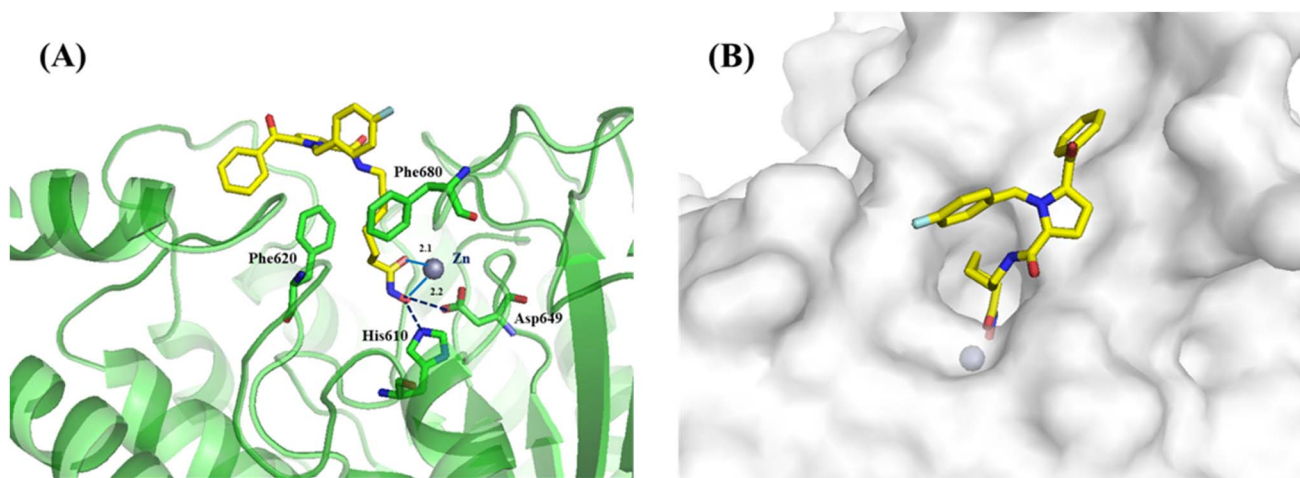

Fig. 3 (A) Binding model of **10g** (yellow) in the catalytic pocket of HDAC6. (B) Surface map of **10g** (yellow) in the catalytic pocket of HDAC6. Key residues were labeled in green. The hydrogen bonds were labeled in blue. Zinc ion was shown in brown.

Table 3 Antiproliferative effect of **10e** and **10g–i** against Hela and SiHa cell lines (IC$_{50}$^{a}, μM)

Compound	Hela	SiHa	HcerEpic
10e	4.40 ± 0.23	7.50 ± 0.44	/^{b}
10g	2.00 ± 0.15	4.60 ± 0.23	>50
10h	3.90 ± 0.20	7.00 ± 0.50	—
10i	2.70 ± 0.09	5.40 ± 0.18	>50
ACY1215	6.80 ± 0.35	11.3 ± 0.80	>50
SAHA	0.58 ± 0.03	3.4 ± 0.11	—

^{a} IC$_{50}$ values are averages of three independent experiments, SD < 10%. ^{b} Not determined.

Table 4 *In vitro* stabilities of compound **10g** and ACY-1215 toward HLM

Compound	HLM concentration	Substrate concentration	$T_{1/2}$
10g	0.8 mg mL^{-1}	0.5 μM	8.5 h
ACY1215	0.8 mg mL^{-1}	0.5 μM	6.7 h

in human normal cervical epithelial cells (HcerEpic). Current data suggested these compounds are promising candidates for cervical cancer treatment.

4.4 Microsomal stability study

ACY-1215 was easily metabolized and cleared *in vivo*, which limits its clinical applications. Hence, preliminary stability study was performed to determinate the half-life ($T_{1/2}$) of **10g** in human liver microsome (HLM). As shown in Table 4, the elimination $T_{1/2}$ value of **10g** was 8.5 h, better than that of ACY-1215 (6.7 h).

5. Conclusion

In this paper, eighteen aroylpyrrole derivatives were designed and synthesized as sHDAC6is based on the well-established pharmacophore, and five aroylpyrroles demonstrated single-digital nanomolar HDAC6 activity. The most potent compound **10g** showed an IC$_{50}$ of 3.9 nM against HDAC6 and 95~fold selectivity over other isoforms including HDAC1/2/3/4/5/8. In cellular assay, **10g** also showed promising result against two cervical cancer cell lines Hela and SiHa. Molecular docking study supported the rationality of compound design, and further modifications could be attempted on the 4-position of pyrrole skeleton in the future experiment. Taken together, this work highlighted the application of aroylpyrrole scaffold in the development of sHDAC6is and these novel aroylpyrroles might be developed as new antitumor agents in the treatment of cervical cancer.

6. Experimental section

6.1 Chemistry

All of the starting reagents were purchased and were used with no additional purification. All of the mentioned yields were for isolated products. Melting points were determined in open capillaries on a WRS-1A digital melting point apparatus (Shenguang). ^{1}H-NMR spectras were detected on a Bruker DRX-400 (400 MHz or 500 MHz) using TMS as internal standard. High resolution mass spectra were obtained from Thermo Scientific Q Exactive. The chemical shifts were reported in ppm (δ) and coupling constants (*J*) values were given in Hertz (Hz). The purities of all target compounds were tested by HPLC to be >95.0%. HPLC analysis was performed at room temperature using an Agilent Eclipse XDB-C18 (250 mm × 4.6 mm) and plotted at 254 nm by 30% MeOH/H$_2$O as a mobile phase.

6.1.1 Methyl 4-benzoyl-1H-pyrrole-2-carboxylate (8). Compound 8 was synthesized according to the literature.[43] To a stirred solution of anhydrous AlCl$_3$ (2.00 g, 14.99 mmol) in 50 mL of anhydrous CH$_2$Cl$_2$ under an argon atmosphere was added was dropwise added benzoyl chloride (0.86 mL, 7.49 mmol). After stirring at −20 °C for 1 h, methyl 2-pyrrole-carboxylate (0.85 g, 6.81 mmol) was added. Then the reaction mixture was stirred for additional 6 h at 40 °C. After the reaction was completed, the mixture was diluted with saturated sodium chloride (100 mL) and extracted with EtOAc (60 mL × 3). The combined organic extracts were dried over anhydrous Na$_2$SO$_4$ and concentrated under reduced pressure. The product was obtained as a pale yellow solid by chromatography on a silica gel column (petroleum ether : ethyl acetate = 4 : 1) in a yield of 95%. ^{1}H NMR (400 MHz, DMSO-d_6) δ 12.75 (s, 1H), 7.80–7.76 (m, 2H), 7.63 (t, *J* = 7.4 Hz, 1H), 7.58 (dd, *J* = 3.3, 1.6 Hz, 1H), 7.54 (t, *J* = 7.5 Hz, 2H), 7.16–7.14 (m, 1H), 3.81 (s, 3H).

6.1.2 General procedure for the synthesis of compounds 9a–j. To a solution of intermediate **8** (0.69 g, 3.00 mmol) and halohydrocarbon (3.50 mmol) in 20 mL DMF was added NaH (0.11 g, 4.50 mmol). The reaction was stirred at room temperature for 8–12 h. After completed, the mixture was quenched with saturated ammonium chloride (5 mL), and additional water (75 mL) was added. The aqueous layer was extracted with ethyl acetate (150 mL × 3) and concentrated under reduced pressure. Purification by column chromatography (petroleum ether/ethyl acetate = 8 : 1) afforded desired products.

6.1.2.1 Methyl 4-benzoyl-1-methyl-1H-pyrrole-2-carboxylate (9a). While solid, 73% yield. ^{1}H NMR (400 MHz, DMSO-d_6) δ 7.97 (d, *J* = 2.0 Hz, 1H), 7.80–7.77 (m, 2H), 7.65–7.61 (m, 1H), 7.53 (t, *J* = 7.4 Hz, 2H), 7.20 (d, *J* = 2.0 Hz, 1H), 4.21 (d, *J* = 7.2 Hz, 2H), 3.91 (s, 3H), 3.73 (s, 3H).

6.1.2.2 Methyl 4-benzoyl-1-(cyclopropylmethyl)-1H-pyrrole-2-carboxylate (9b). While solid, 80% yield. ^{1}H NMR (400 MHz, DMSO-d_6) δ 7.91 (d, *J* = 1.9 Hz, 1H), 7.80–7.77 (m, 2H), 7.66–7.62 (m, 1H), 7.55 (t, *J* = 7.4 Hz, 2H), 7.23 (d, *J* = 2.0 Hz, 1H), 4.22 (d, *J* = 7.2 Hz, 2H), 3.79 (s, 3H), 1.30 (tt, *J* = 7.7, 4.2 Hz, 1H), 0.50–0.45 (m, 2H), 0.38 (q, *J* = 4.9 Hz, 2H).

6.1.2.3 Methyl 4-benzoyl-1-(3-chlorobenzyl)-1H-pyrrole-2-carboxylate (9c). While solid, 71% yield. ^{1}H NMR (400 MHz, DMSO-d_6) δ 8.05 (d, *J* = 2.0 Hz, 1H), 7.78–7.73 (m, 2H), 7.56 (t, *J* = 7.3 Hz, 1H), 7.50 (t, *J* = 7.7 Hz, 2H), 7.25–7.21 (m, 2H), 7.16–7.06 (m, 3H), 5.55 (s, 2H), 3.68 (s, 3H).

6.1.2.4 Methyl 4-benzoyl-1-(4-chlorobenzyl)-1H-pyrrole-2-carboxylate (9d). While solid, 75% yield. ^{1}H NMR (400 MHz, DMSO-d_6) δ 8.03 (d, *J* = 2.0 Hz, 1H), 7.78–7.73 (m, 2H), 7.59 (t, *J*

= 7.2 Hz, 1H), 7.51 (t, *J* = 7.7 Hz, 2H), 7.21–7.17 (m, 2H), 7.16–7.08 (m, 3H), 5.56 (s, 2H), 3.69 (s, 3H).

6.1.2.5 Methyl 4-benzoyl-1-(2-chlorobenzyl)-1H-pyrrole-2-carboxylate (9e). While solid, 69% yield. ^{1}H NMR (400 MHz, DMSO-d_6) δ 8.00 (d, *J* = 2.0 Hz, 1H), 7.76–7.71 (m, 2H), 7.58 (t, *J* = 7.3 Hz, 1H), 7.50 (t, *J* = 7.4 Hz, 2H), 7.20–7.16 (m, 2H), 7.15–7.07 (m, 3H), 5.57 (s, 2H), 3.68 (s, 3H).

6.1.2.6 Methyl 4-benzoyl-1-(4-fluorobenzyl)-1H-pyrrole-2-carboxylate (9f). While solid, 80% yield. ^{1}H NMR (400 MHz, DMSO-d_6) δ 8.02 (d, *J* = 2.0 Hz, 1H), 7.77–7.72 (m, 2H), 7.58 (t, *J* = 7.3 Hz, 1H), 7.49 (t, *J* = 7.7 Hz, 2H), 7.20 (dd, *J* = 9.0, 2.5 Hz, 2H), 7.15–7.05 (m, 3H), 5.54 (s, 2H), 3.67 (s, 3H).

6.1.2.7 Methyl 4-benzoyl-1-(4-(trifluoromethyl)benzyl)-1H-pyrrole-2-carboxylate (9g). While solid, 83% yield. ^{1}H NMR (400 MHz, DMSO-d_6) δ 8.11 (d, *J* = 2.0 Hz, 1H), 7.82 (d, *J* = 7.0 Hz, 2H), 7.78–7.66 (m, 3H), 7.56 (t, *J* = 7.5 Hz, 2H), 7.37–7.28 (m, 3H), 5.72 (s, 2H), 3.71 (s, 3H).

6.1.2.8 Methyl 4-benzoyl-1-benzyl-1H-pyrrole-2-carboxylate (9h). While solid, 79% yield. ^{1}H NMR (400 MHz, DMSO-d_6) δ 7.96 (d, *J* = 2.0 Hz, 1H), 7.76–7.72 (m, 2H), 7.55 (t, *J* = 7.2 Hz, 1H), 7.46 (t, *J* = 7.6 Hz, 2H), 7.23–7.19 (m, 3H), 7.16–7.06 (m, 3H), 5.54 (s, 2H), 3.66 (s, 3H).

6.1.2.9 Methyl 4-benzoyl-1-(3-methoxybenzyl)-1H-pyrrole-2-carboxylate (9i). While solid, 74% yield. ^{1}H NMR (400 MHz, DMSO-d_6) δ 8.01 (d, *J* = 2.0 Hz, 1H), 7.82–7.76 (m, 2H), 7.67–7.61 (m, 1H), 7.55 (t, *J* = 7.4 Hz, 2H), 7.24 (d, *J* = 2.0 Hz, 1H), 7.16–6.89 (m, 2H), 5.55 (s, 2H), 3.74 (s, 3H), 3.70 (s, 3H).

6.1.2.10 Methyl 4-benzoyl-1-(4-methoxybenzyl)-1H-pyrrole-2-carboxylate (9j). While solid, 68% yield. ^{1}H NMR (400 MHz, DMSO-d_6) δ 8.02 (d, *J* = 2.0 Hz, 1H), 7.81–7.75 (m, 2H), 7.67–7.61 (m, 1H), 7.55 (t, *J* = 7.4 Hz, 2H), 7.24 (d, *J* = 2.0 Hz, 1H), 7.17 (d, *J* = 8.7 Hz, 2H), 6.89 (d, *J* = 8.7 Hz, 2H), 5.54 (s, 2H), 3.75 (s, 3H), 3.71 (s, 3H).

6.1.3 General procedure for the synthesis of compounds 10a–k, 11a–g. (i) To a solution of compound 9a (0.42 g, 1.50 mmol) in MeOH (30 mL) was added NaOH (0.24 g, 6.00 mmol). Then, the reaction was stirred for 18 hours at 60 °C. After the reaction was completed, the solvent was concentrated under reduced pressure. After diluted with water (10 mL), 30% hydrochloric acid (30 mL) was added dropwise to adjust the pH = 7. The filter cake was collected and dried for next step; (ii) To a solution of product from step I (1.35 mmol), DIPEA (1 mL, 5.4 mmol) and HATU (0.57 g, 1.5 mmol) in DMF (20 mL) was added methyl 4-(aminomethyl)benzoate (0.22 g, 1.35 mmol), methyl 7-aminoheptanoate (0.215 g, 1.35 mmol) or methyl 6-amino-hexanoate (0.196 g, 1.35 mmol) at 0 °C. The reaction was stirred for 6 hours. The mixture was poured in water (150 mL) and extracted with ethyl acetate (100 mL × 3). Purification by column chromatography (petroleum ether/ethyl acetate = 1 : 2) afforded compound for next step; (iii) To a solution of NH$_2$OH HCl (1.70 g, 24.46 mmol) in MeOH (9 mL) was added with KOH (1.70 g, 30.29 mmol) at 0 °C in an ice bath. Then the mixture was stirred for 30 min and filtered. Product from step ii was added to the filtrate and the reaction was stirred for an additional 4 h at 0 °C. The resulting mixture was poured into water (30 mL) and pH value was adjusted to 7. The mixture was diluted with saturated NaCl aqueous solution (40 mL) and extracted with

EtOAc (50 mL × 3). After dried over Na$_2$SO$_4$, the organic phase was concentrated and purified by column chromatography to give the target compounds.

6.1.3.1 5-Benzoyl-N-(7-(hydroxyamino)-7-oxoheptyl)-1-methyl-1H-pyrrole-2-carboxamide (10a). White solid, yield 60.5%, m.p.: 101.3 ∼ 102.5 °C. ^{1}H NMR (400 MHz, DMSO-d_6) δ 11.32 (s, 1H), 10.34 (s, 1H), 8.67 (s, 1H), 8.09 (q, *J* = 5.4 Hz, 1H), 7.55 (d, *J* = 1.8 Hz, 1H), 7.43 (dt, *J* = 7.2, 5.2 Hz, 4H), 6.90 (d, *J* = 1.9 Hz, 1H), 3.86 (s, 3H), 3.11 (p, *J* = 6.6 Hz, 2H), 1.92 (td, *J* = 7.4, 3.4 Hz, 2H), 1.44 (dt, *J* = 14.8, 7.4 Hz, 4H), 1.22 (dd, *J* = 9.0, 4.3 Hz, 4H). ^{13}C NMR (101 MHz, DMSO-d_6) δ 169.17, 161.01, 151.13, 150.19, 137.62, 134.12, 131.63, 128.65, 128.55, 128.33, 128.15, 127.96, 127.16, 126.58, 125.16, 119.50, 113.88, 113.38, 109.83, 38.44, 36.52, 32.28, 29.19, 28.38, 26.27, 25.15. IR (KBr, cm^{-1}): 3218.3, 2928.1, 2857.0, 1651.9, 1557.1, 1527.5, 1293.6, 769.5, 701.4. HRMS (ESI) *m/z* calcd for C$_{20}$H$_{25}$N$_3$O$_4$Na$^+$ (M + Na)$^+$ 394.17373, found 394.17365.

6.1.3.2 5-Benzoyl-1-(cyclopropylmethyl)-N-(7-(hydroxyamino)-7-oxoheptyl)-1H-pyrrole-2-carboxamide (10b). White solid, yield 66.0%, m.p.: 107.0 ∼ 109.0 °C. ^{1}H NMR (400 MHz, DMSO-d_6) δ 11.32 (s, 1H), 10.33 (s, 1H), 8.67 (s, 1H), 8.11 (t, *J* = 6.1 Hz, 1H), 7.67–7.58 (m, 1H), 7.49–7.35 (m, 4H), 6.92–6.78 (m, 1H), 4.21 (dd, *J* = 11.5, 7.1 Hz, 2H), 3.11 (q, *J* = 6.5 Hz, 2H), 1.91 (t, *J* = 7.2 Hz, 2H), 1.45 (d, *J* = 6.9 Hz, 4H), 1.23 (s, 4H), 0.84 (d, *J* = 6.9 Hz, 1H), 0.46–0.38 (m, 2H), 0.33–0.21 (m, 2H). ^{13}C NMR (101 MHz, DMSO-d_6) δ 193.61, 182.40, 179.06, 169.15, 161.15, 150.23, 137.64, 130.61, 128.66, 128.58, 128.54, 128.31, 128.14, 127.95, 124.59, 114.12, 113.47, 52.22, 38.43, 32.27, 29.18, 28.38, 26.24, 25.16, 12.75, 3.45, 3.38. IR (KBr, cm^{-1}): 3223.4, 2924.9, 2851.8, 1633.5, 1551.3, 1523.9, 1292.4, 1240.6, 698.5. HRMS (ESI) *m/z* calcd for C$_{23}$H$_{29}$N$_3$O$_4$Na$^+$ (M + Na)$^+$ 434.20503, found 434.20508.

6.1.3.3 5-Benzoyl-1-(3-chlorobenzyl)-N-(6-(hydroxyamino)-6-oxohexyl)-1H-pyrrole-2-carboxamide (10c). Yellow solid, yield 63.3%, m.p.: 104.6 ∼ 106.2 °C. ^{1}H NMR (400 MHz, DMSO-d_6) δ 11.40 (s, 1H), 10.32 (s, 1H), 8.15 (q, *J* = 5.5 Hz, 1H), 7.78 (d, *J* = 1.7 Hz, 1H), 7.47–7.44 (m, 2H), 7.43–7.41 (m, 3H), 7.34–7.28 (m, 3H), 7.16 (s, 1H), 6.93 (d, *J* = 1.7 Hz, 1H), 5.63 (s, 2H), 1.40 (dt, *J* = 24.4, 6.4 Hz, 6H), 1.24–1.14 (m, 6H). ^{13}C NMR (101 MHz, DMSO-d_6) δ 160.88, 150.02, 141.68, 137.45, 133.00, 130.32, 128.62, 128.15, 126.77, 125.66, 124.61, 114.45, 114.06, 32.25, 29.09, 28.34, 26.13, 25.09. IR (KBr, cm^{-1}): 3203.5, 2931.0, 2857.0, 1640.0, 1557.1, 1426.8, 1293.6, 769.5, 698.4. HRMS (ESI) *m/z* calcd for C$_{26}$H$_{28}$Cl^{35}N$_3$O$_4$Na$^+$ (M + Na)$^+$ 504.16606, found 504.16660.

6.1.3.4 5-Benzoyl-1-(3-chlorobenzyl)-N-(7-(hydroxyamino)-7-oxoheptyl)-1H-pyrrole-2-carboxamide (10d). Yellow solid, yield: 56.2%, m.p.: 122.9 ∼ 124.3 °C. ^{1}H NMR (400 MHz, DMSO-d_6) δ 11.40 (s, 1H), 10.32 (s, 1H), 8.66 (s, 1H), 8.15 (t, *J* = 5.7 Hz, 1H), 7.78 (d, *J* = 1.6 Hz, 1H), 7.48–7.44 (m, 2H), 7.44–7.41 (m, 3H), 7.31 (dd, *J* = 3.7, 2.0 Hz, 1H), 7.17 (s, 1H), 7.09 (d, *J* = 7.2 Hz, 1H), 6.94 (d, *J* = 1.3 Hz, 1H), 5.64 (s, 2H), 3.07 (q, *J* = 6.6 Hz, 2H), 1.90 (t, *J* = 7.4 Hz, 2H), 1.49–1.43 (m, 2H), 1.38 (q, *J* = 7.3 Hz, 2H), 1.21–1.14 (m, 2H). ^{13}C NMR (101 MHz, DMSO-d_6) δ 169.17, 160.93, 150.08, 141.72, 137.50, 133.06, 130.35, 128.67, 128.20, 128.01, 127.17, 126.81, 125.69, 124.65, 114.52, 114.11, 50.33, 38.43, 32.31, 29.14, 28.40, 26.19, 25.17, 25.15. IR (KBr, cm^{-1}): 3218.3, 2928.1, 2857.0, 1640.0, 1557.1, 1290.6, 1133.7, 769.5,

695.4. HRMS (ESI) m/z calcd for $C_{25}H_{26}Cl_{35}N_3O_4Na^+$ (M + Na)$^+$ 490.15041, found 490.15079.

6.1.3.5 5-Benzoyl-1-(4-chlorobenzyl)-N-(7-(hydroxyamino)-7-oxoheptyl)-1H-pyrrole-2-carboxamide (10e). Yellow solid, yield 59.5%, m.p.: 142.2 ∼ 143.7 °C. ^{1}H NMR (400 MHz, DMSO-d_6) δ 11.98 (s, 1H), 10.94 (s, 1H), 9.28 (s, 1H), 8.70 (s, 1H), 8.05–7.95 (m, 4H), 7.94–7.86 (m, 3H), 7.69 (dd, J = 19.2, 8.1 Hz, 2H), 7.56–7.51 (m, 1H), 6.19 (s, 2H), 3.74 (dd, J = 5.3, 2.2 Hz, 2H), 3.66 (t, J = 6.8 Hz, 2H), 2.05–1.91 (m, 4H), 1.80–1.72 (m, 4H). ^{13}C NMR (101 MHz, DMSO-d_6) δ 169.25, 160.94, 150.14, 138.23, 137.54, 131.86, 128.90, 128.83, 128.72, 128.63, 128.42, 128.37, 128.22, 128.03, 124.67, 120.34, 114.12, 48.71, 38.46, 32.34, 29.16, 28.41, 26.23, 25.18. IR (KBr, cm^{-1}): 3202.0, 2931.0, 2854.8, 1639.6, 1554.3, 1523.9, 1292.4, 698.5. HRMS (ESI) m/z calcd for $C_{21}H_{19}N_3O_4Na^+$ (M + Na)$^+$ 504.16606, found 504.16681.

6.1.3.6 5-Benzoyl-1-(2-chlorobenzyl)-N-(7-(hydroxyamino)-7-oxoheptyl)-1H-pyrrole-2-carboxamide (10f). Yellow solid, yield: 66.4%, m.p.: 152.1 ∼ 153.9 °C. ^{1}H NMR (400 MHz, DMSO-d_6) δ 11.39 (s, 1H), 10.32 (s, 1H), 8.58 (s, 1H), 8.25–8.02 (m, 1H), 7.84–7.58 (m, 1H), 7.51–7.39 (m, 5H), 7.26 (dt, J = 12.7, 6.6 Hz, 2H), 7.03 (t, J = 2.1 Hz, 1H), 6.48 (dd, J = 21.6, 9.4 Hz, 1H), 5.73 (s, 2H), 3.04 (q, J = 6.5 Hz, 2H), 1.90 (t, J = 7.3 Hz, 2H), 1.38 (dt, J = 27.5, 5.4 Hz, 4H), 1.22–1.09 (m, 4H). ^{13}C NMR (101 MHz, DMSO-d_6) δ 169.17, 160.73, 160.70, 150.91, 150.07, 137.47, 137.19, 137.05, 133.88, 131.58, 131.11, 130.99, 129.14, 129.08, 128.74, 128.70, 128.64, 128.62, 128.43, 128.21, 128.00, 127.53, 127.14, 126.97, 126.38, 124.93, 120.39, 114.42, 114.18, 110.59, 49.28, 49.17, 48.67, 38.38, 32.28, 29.12, 28.36, 26.18, 25.14. IR (KBr, cm^{-1}): 3211.2, 2927.9, 2854.8, 1636.5, 1554.3, 1438.6, 1292.4, 695.4. HRMS (ESI) m/z calcd for $C_{26}H_{28}Cl_{35}N_3O_4Na^+$ (M + Na)$^+$ 504.16606, found 504.16638.

6.1.3.7 5-Benzoyl-1-(4-fluorobenzyl)-N-(7-(hydroxyamino)-7-oxoheptyl)-1H-pyrrole-2-carboxamide (10g). White solid, yield: 57.1%, m.p.: 119.9 ∼ 121.9 °C. ^{1}H NMR (400 MHz, DMSO-d_6) δ 11.39 (s, 1H), 10.35 (s, 1H), 8.69 (s, 1H), 8.13 (dt, J = 11.3, 5.7 Hz, 1H), 7.77 (d, J = 1.8 Hz, 1H), 7.47–7.39 (m, 4H), 7.27–7.05 (m, 4H), 6.92 (d, J = 2.4 Hz, 1H), 5.61 (s, 2H), 3.09 (q, J = 6.6 Hz, 2H), 2.01–1.84 (m, 2H), 1.51–1.35 (m, 4H), 1.24–1.18 (m, 4H). ^{13}C NMR (101 MHz, DMSO-d_6) δ 169.24, 161.02, 160.23, 150.14, 137.53, 135.37, 131.04, 129.28, 129.13, 128.61, 128.41, 128.22, 128.04, 124.64, 120.26, 115.32, 115.11, 114.49, 114.06, 50.14, 38.45, 32.31, 29.15, 28.39, 26.21, 25.17. IR (KBr, cm^{-1}): 3220.3, 2927.9, 2851.8, 1627.4, 1557.4, 1508.6, 768.5, 695.4. HRMS (ESI) m/z calcd for $C_{26}H_{28}FN_3O_4Na^+$ (M + Na)$^+$ 488.19561, found 488.19598.

6.1.3.8 5-Benzoyl-N-(7-(hydroxyamino)-7-oxoheptyl)-1-(4-(trifluoromethyl)benzyl)-1H-pyrrole-2-carboxamide (10h). Yellow solid, yield: 55%, m.p.: 138.1 ∼ 139.8 °C. ^{1}H NMR (400 MHz, DMSO-d_6) δ 11.41 (s, 1H), 10.32 (s, 1H), 8.66 (s, 1H), 8.14 (dt, J = 11.4, 5.9 Hz, 1H), 7.80 (s, 1H), 7.66 (t, J = 8.7 Hz, 2H), 7.45 (dd, J = 15.7, 5.2 Hz, 4H), 7.25 (dd, J = 18.3, 8.0 Hz, 2H), 6.98 (s, 1H), 5.73 (s, 2H), 3.06 (t, J = 6.7 Hz, 2H), 1.90 (t, J = 7.3 Hz, 2H), 1.39 (dt, J = 29.7, 7.2 Hz, 4H), 1.18 (s, 4H). ^{13}C NMR (101 MHz, DMSO-d_6) δ 188.90, 169.10, 160.71, 158.66, 139.02, 132.47, 131.80, 130.37, 128.97, 128.56, 128.54, 126.97, 121.73, 113.82, 55.06, 50.57, 32.27, 29.03, 28.37, 26.16, 25.13. IR (KBr, cm^{-1}): 3218.3, 2934.0, 2857.0, 1640.0, 1557.1, 1527.5, 769.5, 701.4.

HRMS (ESI) m/z calcd for $C_{27}H_{28}F_3N_3O_4Na^+$ (M + Na)$^+$ 538.19241, found 538.19241.

6.1.3.9 5-Benzoyl-1-benzyl-N-(7-(hydroxyamino)-7-oxoheptyl)-1H-pyrrole-2-carboxamide (10i). Yellow solid, yield: 61.8%, m.p.: 151.7 ∼ 153.1 °C. ^{1}H NMR (400 MHz, DMSO-d_6) δ 10.35 (s, 1H), 8.69 (s, 1H), 8.30 (t, J = 5.7 Hz, 1H), 7.87–7.68 (m, 3H), 7.58 (dt, J = 34.3, 7.4 Hz, 3H), 7.27 (dq, J = 14.5, 7.0 Hz, 4H), 7.17 (d, J = 6.9 Hz, 2H), 5.65 (s, 2H), 3.12 (q, J = 6.6 Hz, 2H), 1.92 (t, J = 7.3 Hz, 2H), 1.50–1.36 (m, 4H), 1.21 (dq, J = 7.7, 4.1 Hz, 4H). ^{13}C NMR (101 MHz, DMSO-d_6) δ 188.96, 169.14, 160.63, 139.02, 138.51, 132.84, 131.84, 128.59, 128.57, 128.49, 127.42, 127.18, 127.11, 121.82, 113.81, 38.47, 32.29, 29.01, 28.37, 26.14, 25.14. IR (KBr, cm^{-1}): 3351.5, 2957.7, 2925.1, 1672.6, 1628.2, 1018.2, 796.1. HRMS (ESI) m/z calcd for $C_{26}H_{29}N_3O_4Na^+$ (M + Na)$^+$ 470.20503, found 470.20508.

6.1.3.10 5-Benzoyl-N-(7-(hydroxyamino)-7-oxoheptyl)-1-(3-methoxybenzyl)-1H-pyrrole-2-carboxamide (10j). White solid, yield: 63.5%, m.p.: 153.1∼154.8 °C. ^{1}H NMR (400 MHz, DMSO-d_6) δ 10.35 (s, 1H), 8.68 (s, 1H), 8.32 (t, J = 5.7 Hz, 1H), 7.84–7.73 (m, 3H), 7.62 (t, J = 7.4 Hz, 1H), 7.54 (t, J = 7.5 Hz, 2H), 7.27 (d, J = 1.9 Hz, 1H), 7.21 (t, J = 7.9 Hz, 1H), 6.81 (d, J = 8.1 Hz, 1H), 6.77–6.70 (m, 2H), 5.62 (s, 2H), 3.69 (s, 3H), 3.13 (q, J = 6.7 Hz, 2H), 1.92 (t, J = 7.4 Hz, 2H), 1.50–1.38 (m, 4H), 1.22 (q, J = 3.6 Hz, 4H). ^{13}C NMR (101 MHz, DMSO-d_6) δ 188.94, 169.14, 160.68, 159.33, 140.06, 139.01, 132.82, 131.83, 129.62, 128.58, 128.55, 127.15, 121.82, 119.28, 113.78, 113.13, 112.52, 54.99, 51.09, 38.50, 32.29, 29.03, 28.38, 26.16, 25.12. IR (KBr, cm^{-1}): 3241.6, 2931.0, 2854.8, 1630.5, 1560.4, 1289.3, 725.9. HRMS (ESI) m/z calcd for $C_{27}H_{31}N_3O_5Na^+$ (M + Na)$^+$ 500.21559, found 500.21548.

6.1.3.11 5-Benzoyl-N-(7-(hydroxyamino)-7-oxoheptyl)-1-(4-methoxybenzyl)-1H-pyrrole-2-carboxamide (10k). Yellow solid, yield: 61.9%, m.p.: 158.5 ∼ 159.9 °C. ^{1}H NMR (400 MHz, DMSO-d_6) δ 10.34 (s, 1H), 8.67 (s, 1H), 8.28 (t, J = 5.7 Hz, 1H), 7.83–7.73 (m, 3H), 7.62 (t, J = 7.3 Hz, 1H), 7.54 (t, J = 7.4 Hz, 2H), 7.24 (d, J = 1.9 Hz, 1H), 7.19 (d, J = 8.7 Hz, 2H), 6.85 (d, J = 8.7 Hz, 2H), 5.56 (s, 2H), 3.70 (s, 3H), 3.17–3.12 (m, 2H), 1.93 (t, J = 7.3 Hz, 2H), 1.44 (dd, J = 13.1, 5.9 Hz, 4H), 1.23 (s, 4H). ^{13}C NMR (101 MHz, DMSO-d_6) δ 188.90, 169.10, 160.71, 158.66, 139.02, 132.47, 131.80, 130.37, 128.97, 128.56, 128.54, 126.97, 121.73, 113.82, 55.06, 50.57, 32.27, 29.03, 28.37, 26.16, 25.13. IR (KBr, cm^{-1}): 3241.6, 2931.0, 2854.8, 1630.5, 1560.4, 1289.4, 725.9. HRMS (ESI) m/z calcd for $C_{27}H_{31}N_3O_5Na^+$ (M + Na)$^+$ 500.21559, found 500.21552.

6.1.3.12 5-Benzoyl-N-(4-(hydroxycarbamoyl)benzyl)-1-methyl-1H-pyrrole-2-carboxamide (11a). White solid, yield 51.2%, m.p.: 137.3 ∼ 138.9 °C. ^{1}H NMR (400 MHz, DMSO-d_6) δ 11.35 (s, 1H), 11.16 (s, 1H), 8.71 (t, J = 6.0 Hz, 1H), 7.68 (d, J = 8.1 Hz, 2H), 7.59 (s, 1H), 7.47–7.40 (m, 5H), 7.32 (d, J = 8.1 Hz, 2H), 7.04–7.01 (m, 1H), 4.37 (d, J = 5.9 Hz, 2H), 3.88 (s, 3H). ^{13}C NMR (101 MHz, DMSO-d_6) δ 161.11, 150.12, 143.32, 137.55, 132.06, 131.22, 128.66, 128.35, 128.16, 127.07, 126.92, 124.62, 114.39, 113.56, 48.65, 41.69, 36.65. IR (KBr, cm^{-1}): 3216.2, 2923.8, 2851.1, 1637.1, 1546.1, 1296.5, 766.5, 698.4. HRMS (ESI) m/z calcd for $C_{21}H_{19}N_3O_4Na^+$ (M + Na)$^+$ 400.12678, found 400.12628.

6.1.3.13 5-Benzoyl-1-(cyclopropylmethyl)-N-(4-(hydroxycarbamoyl)benzyl)-1H-pyrrole-2-carboxamide (11b). White solid, yield 62.5%, m.p.: 138.9 ∼ 140.5 °C. ^{1}H NMR (400 MHz, DMSO-

d_6) δ 11.35 (s, 1H), 11.16 (s, 1H), 8.73 (t, J = 6.1 Hz, 1H), 7.68 (d, J = 8.0 Hz, 3H), 7.46 (dd, J = 6.7, 3.2 Hz, 2H), 7.44–7.40 (m, 3H), 7.32 (d, J = 8.2 Hz, 2H), 7.01 (d, J = 1.6 Hz, 1H), 4.38 (d, J = 6.0 Hz, 2H), 4.22 (d, J = 7.1 Hz, 2H), 1.23 (s, 1H), 0.42 (d, J = 9.5 Hz, 2H), 0.30 (d, J = 4.9 Hz, 2H). ^{13}C NMR (101 MHz, DMSO-d_6) δ 161.32, 150.25, 143.40, 137.61, 131.23, 131.13, 128.73, 128.43, 128.25, 127.09, 126.98, 126.76, 124.09, 114.74, 113.76, 52.42, 41.78, 21.32, 18.89, 12.81, 3.54. IR (KBr, cm^{-1}): 3221.2, 2925.1, 2848.1, 1634.1, 1551.2, 1284.7, 1142.6, 769.5, 698.4. HRMS (ESI) m/z calcd for $C_{24}H_{23}N_3O_4Na^+$ (M + Na)$^+$ 440.15808, found 440.15805.

6.1.3.14   5-Benzoyl-1-(3-chlorobenzyl)-N-(4-(hydroxycarbamoyl)benzyl)-1H-pyrrole-2-carboxamide (11c). Yellow sold, yield 58%, m.p.: 154.1 ∼ 155.7 °C. ^{1}H NMR (400 MHz, DMSO-d_6) δ 11.43 (s, 1H), 11.16 (s, 1H), 8.99 (s, 1H), 8.78 (dt, J = 12.2, 6.1 Hz, 1H), 7.84 (d, J = 1.6 Hz, 1H), 7.65 (dd, J = 8.2, 3.6 Hz, 2H), 7.49–7.38 (m, 5H), 7.33 (d, J = 5.8 Hz, 2H), 7.23–7.19 (m, 2H), 7.06 (dd, J = 8.5, 6.8 Hz, 2H), 5.65 (s, 2H), 4.35 (t, J = 6.3 Hz, 2H). ^{13}C NMR (101 MHz, DMSO-d_6) δ 161.04, 149.98, 143.10, 141.66, 137.41, 133.10, 133.06, 131.63, 130.38, 130.33, 128.65, 128.58, 128.41, 128.20, 128.03, 127.20, 126.88, 126.82, 126.70, 126.63, 125.62, 124.15, 115.09, 114.28, 50.47, 41.64. IR (KBr, cm^{-1}): 3230.1, 2925.1, 2854.1, 1643.0, 1548.2, 1524.5, 1293.6, 1133.7, 772.4, 692.5. HRMS (ESI) m/z calcd for $C_{27}H_{22}Cl_{35}N_3O_4Na^+$ (M + Na)$^+$ 510.11911, found 510.11963.

6.1.3.15   5-Benzoyl-1-(4-fluorobenzyl)-N-(4-(hydroxycarbamoyl)benzyl)-1H-pyrrole-2-carboxamide (11d). White solid, yield 70.3%, m.p.: 126.3 ∼ 127.8 °C. ^{1}H NMR (400 MHz, DMSO-d_6) δ 11.18 (s, 1H), 8.76 (dt, J = 12.3, 6.1 Hz, 1H), 7.83 (d, J = 1.8 Hz, 1H), 7.67 (dd, J = 8.1, 3.9 Hz, 2H), 7.50–7.29 (m, 5H), 7.26–6.98 (m, 7H), 5.63 (s, 2H), 4.35 (d, J = 6.0 Hz, 2H). ^{13}C NMR (101 MHz, DMSO-d_6) δ 164.13, 160.89, 149.94, 143.96, 143.06, 137.40, 131.76, 128.65, 128.56, 128.36, 128.17, 127.54, 127.36, 126.89, 126.83, 125.35, 125.31, 124.12, 115.06, 114.32, 50.73, 41.60. IR (KBr, cm^{-1}): 3259.9, 2924.9, 2854.8, 1639.6, 1603.0, 1542.1, 1508.6, 1301.5, 768.5, 701.5. HRMS (ESI) m/z calcd for $C_{27}H_{22}FN_3O_4Na^+$ (M + Na)$^+$ 494.14866, found 494.14871.

6.1.3.16   5-Benzoyl-N-(4-(hydroxycarbamoyl)benzyl)-1-(4-(trifluoromethyl)benzyl)-1H-pyrrole-2-carboxamide (11e). White solid, yield 63.4%, m.p.: 120.6 ∼ 122.0 °C. ^{1}H NMR (400 MHz, DMSO-d_6) δ 11.15 (s, 1H), 8.99 (s, 1H), 8.76 (t, J = 6.2 Hz, 1H), 7.88–7.79 (m, 1H), 7.70–7.61 (m, 4H), 7.58–7.45 (m, 2H), 7.45–7.31 (m, 3H), 7.30–7.16 (m, 4H), 7.13–7.01 (m, 1H), 5.75 (s, 2H), 4.33 (s, 2H). ^{13}C NMR (101 MHz, DMSO-d_6) δ 161.09, 149.99, 143.13, 137.43, 135.24, 135.21, 131.40, 131.21, 129.22, 129.16, 129.14, 128.64, 128.15, 126.92, 126.87, 126.84, 124.10, 115.27, 115.22, 115.06, 115.00, 114.15, 50.19, 41.64. IR (KBr, cm^{-1}): 3256.9, 3055.8, 2924.9, 2851.8, 1633.5, 1551.3, 1526.9, 1325.9, 768.5, 698.5. HRMS (ESI) m/z calcd for $C_{28}H_{22}F_3N_3O_4Na^+$ (M + Na)$^+$ 544.14546, found 544.14551.

6.1.3.17   5-Benzoyl-1-benzyl-N-(4-(hydroxycarbamoyl)benzyl)-1H-pyrrole-2-carboxamide (11f). White solid, yield 59.3%, m.p.: 121.5 ∼ 122.8 °C. ^{1}H NMR (400 MHz, DMSO-d_6) δ 11.20 (s, 1H), 9.03 (s, 1H), 8.94 (t, J = 6.1 Hz, 1H), 7.89 (d, J = 1.9 Hz, 1H), 7.83–7.76 (m, 2H), 7.71–7.58 (m, 3H), 7.54 (dd, J = 8.1, 6.7 Hz, 2H), 7.38 (d, J = 1.9 Hz, 1H), 7.34–7.20 (m, 5H), 7.19–7.11 (m, 2H), 5.67 (s, 2H), 4.40 (d, J = 6.0 Hz, 2H). ^{13}C NMR (101 MHz, DMSO-

d_6) δ 188.93, 164.15, 160.83, 142.91, 138.96, 138.43, 133.21, 131.89, 131.26, 128.62, 128.58, 128.52, 127.46, 127.17, 126.94, 126.92, 126.66, 121.94, 114.42, 51.38, 41.72. IR (KBr, cm^{-1}): 3247.5, 2923.9, 2851.5, 1640.9, 1549.5, 1290.6, 719.5. HRMS (ESI) m/z calcd for $C_{27}H_{23}N_3O_4Na^+$ (M + Na)$^+$ 476.15808, found 476.15811.

6.1.3.18   5-Benzoyl-N-(4-(hydroxycarbamoyl)benzyl)-1-(4-methoxybenzyl)-1H-pyrrole-2-carboxamide (11g). White solid, yield 63.0%, m.p.: 125.0 ∼ 127.0 °C. ^{1}H NMR (400 MHz, DMSO-d_6) δ 11.18 (s, 1H), 9.00 (s, 1H), 8.92 (t, J = 6.1 Hz, 1H), 7.85 (d, J = 1.9 Hz, 1H), 7.82–7.75 (m, 2H), 7.68 (d, J = 8.2 Hz, 2H), 7.65–7.60 (m, 1H), 7.54 (dd, J = 8.1, 6.8 Hz, 2H), 7.33 (d, J = 1.8 Hz, 1H), 7.27 (d, J = 8.1 Hz, 2H), 7.20–7.11 (m, 2H), 6.87–6.78 (m, 2H), 5.57 (s, 2H), 4.41 (d, J = 6.0 Hz, 2H), 3.72 (s, 3H). ^{13}C NMR (101 MHz, DMSO-d_6) δ 161.20, 159.36, 150.07, 143.21, 140.68, 137.49, 131.58, 129.58, 128.67, 128.40, 128.20, 126.94, 126.89, 124.37, 119.12, 114.93, 114.11, 112.96, 112.31, 54.96, 54.95, 48.67, 41.67, 19.52. IR (KBr, cm^{-1}): 3272.1, 3052.8, 2918.8, 2854.8, 1630.5, 1548.2, 1511.7, 1292.4, 707.6. HRMS (ESI) m/z calcd for $C_{28}H_{25}N_3O_5Na^+$ (M + Na)$^+$ 506.16864, found 506.16882.

6.2   *In vitro* HDAC enzyme assay

IC_{50} testing of compounds were performed by Reaction Biology Corporation. The HDACs were isolated from a baculovirus expression system in Sf9 cells using an acetylated fluorogenic peptide $RHKK_{Ac}$ as substrate. The reaction buffer was made up of 50 mM Tris–HCl pH 8.0, 127 mM NaCl, 2.7 mM KCl, 1 mM $MgCl_2$, 1 mg mL^{-1} BSA, and a final concentration of 1% DMSO. Compounds were delivered in DMSO and delivered to enzyme mixture with preincubation of 5–10 min followed by substrate addition and incubation for 2 h at 30 °C. Trichostatin A and a developer were added to quench the reaction and generate fluorescence, respectively. Dose-response curves were generated starting at 30 μM compound with 3-fold serial dilutions to generate a 10-dose plot. IC_{50} values were then generated from the resulting plots.

6.3   Cell culture and antiproliferative assay

The cells were cultured in IMDM medium with 20% FBS, 100 U/mL penicillin and 100 μg mL^{-1} streptomycin. All cells were maintained at 37 °C in a humidified atmosphere of 5% CO_2 in air. Briefly, 100 μL cell suspension or completed medium were plated into 96-well plate. The compounds were serially diluted to concentrations of 20, 10, 5, 2.5, 1.25, 0.625 μM for SiHa cells and 10, 5, 2.5, 1.25, 0.625 0.313 μM for Hela cells. Compounds were added and incubated for 72 h; Then, 22 μL Alamar blue solution (1 mM) were pipetted into each well of 96-well plate; and the plate was incubated for an additional 5 ∼ 6 h. The absorbance (OD) was read at 530/590 nm. Data were normalized to vehicle groups (DMSO) and represented as the means of three independent measurements with standard errors of <20%. The IC_{50} values were calculated using Prism 5.0.

6.4   Computational methods

Molecular docking was performed using Sybyl-X 2.0 software (222 S Central Ave Ste 1008, Saint Louis, MO 63105, USA) based

on the cocrystal of HDAC6 (PDB: 5EDU). The cavity occupied by trichostatin A was selected as the ligand binding site. Water molecules outside the binding pocket were excluded. The other docking parameters were kept as default.

6.5 Microsomal stability assay

Human liver microsome was provided by Research Institute for Liver Disease (Shanghai) Co., Ltd Briefly, each incubated mixture contained 0.8 mg mL^{-1} HLM, 50 mL magnesium chloride, 60 mL potassium phosphate buffer (pH 7.4) and 0.5 mM test compound in a total volume of 200 mL. After pre-warming at 37 °C for 5 min, 50 mL NADPH was added to initiate the reaction. The reaction was terminated after 0, 5, 10, 15, 30, 60 or 90 min by adding 400 mL ice-cold ethyl acetate into 200 mL of incubation mixture. The sample was then centrifuged at 4000 rpm for 10 min at 4 °C. The supernatant was then analyzed by LC-MS/MS.

Author contributions

Conceptualisation: Xin Chen and Lu Zong; methodology: Xingjie Wang, Wenli Gou and Lixuan Du, Lu Zong; validation: Yaxin Xue, Yitong Su and Xuetao Yuan; formal analysis: Shuting Yang, Weiyi Su and Xingjie Wang; writing-original draft preparation: Lu Zong and Xingjie Wang. Writing—review and editing: Xin Chen and Wenli Gou. All authors have read and agreed to the published version of the manuscript.

Conflicts of interest

The authors declare that they have no known competing financial interests or personal relationships that could have appeared to influence the work reported in this paper.

Data availability

The data supporting this article have been included as part of the supplementary information (SI). Supplementary information is available. See DOI: https://doi.org/10.1039/d5ra06970j.

Acknowledgements

References

1 M. Shvedunova and A. Akhtar, *Nat. Rev. Mol. Cell Biol.*, 2022, **23**, 329–349.

2 V. E. MacDonald and L. J. Howe, *Epigenetics*, 2009, **4**, 139–143.

3 S. Minucci and P. G. Pelicci, *Nat. Rev. Cancer*, 2006, **6**, 38–51.

4 T. Liang, Z. Xie, B. Dang, J. Wang, T. Zhang, X. Luan, T. Lu, C. Cao and X. Chen, *Bioorg. Med. Chem. Lett.*, 2023, **81**, 129148.

5 K. J. Falkenberg and R. W. Johnstone, *Nat. Rev. Drug Discovery*, 2014, **13**, 673–691.

6 J. E. Bolden, M. J. Peart and R. W. Johnstone, *Nat. Rev. Drug Discovery*, 2006, **5**, 769–784.

7 J. J. McClure, X. Li and C. J. Chou, *Adv. Cancer Res.*, 2018, **138**, 183–211.

8 P. A. Marks and R. Breslow, *Nat. Biotechnol.*, 2007, **25**, 84–90.

9 A. Sawas, D. Radeski and O. A. O'Connor, *Ther. Adv. Hematol.*, 2015, **6**, 202–208.

10 J. P. Laubach, P. Moreau, J. F. San-Miguel and P. G. Richardson, *Clin. Cancer Res.*, 2015, **21**, 4767–4773.

11 M. Dong, Z. Q. Ning, P. Y. Xing, J. L. Xu, H. X. Cao, G. F. Dou, Z. Y. Meng, Y. K. Shi, X. P. Lu and F. Y. Feng, *Cancer Chemother. Pharmacol.*, 2012, **69**, 1413–1422.

12 Z. Q. Ning, Z. B. Li, M. J. Newman, S. Shan, X. H. Wang, D. S. Pan, J. Zhang, M. Dong, X. Du and X. P. Lu, *Cancer Chemother. Pharmacol.*, 2012, **69**, 901–909.

13 J. Shi, J. Wang, X. Wang, C. Qu, C. Ye, X. Li, X. Chen and Z. Xu, *RSC Adv.*, 2024, **14**, 12762–12771.

14 I. V. Gregoretti, Y. M. Lee and H. V. Goodson, *J. Mol. Biol.*, 2004, **338**, 17–31.

15 J. H. Kalin and J. A. Bergman, *J. Med. Chem.*, 2013, **56**, 6297–6313.

16 P. LoPresti, *Cells*, 2020, 10.

17 N. Govindarajan, P. Rao, S. Burkhardt, F. Sananbenesi, O. M. Schluter, F. Bradke, J. Lu and A. Fischer, *EMBO Mol. Med.*, 2013, **5**, 52–63.

18 O. Witt, H. E. Deubzer, T. Milde and I. Oehme, *Cancer Lett.*, 2009, **277**, 8–21.

19 P. H. Yang, L. Zhang, Y. J. Zhang, J. Zhang and W. F. Xu, *Drug Discoveries Ther.*, 2013, **7**, 233–242.

20 Y. Zhao, T. Liang, X. Hou and H. Fang, *Curr. Med. Chem.*, 2021, **28**, 4133–4151.

21 X. Chen, X. Chen, R. R. Steimbach, T. Wu, H. Li, W. Dan, P. Shi, C. Cao, D. Li, A. K. Miller, Z. Qiu, J. Gao and Y. Zhu, *Eur. J. Med. Chem.*, 2020, **187**, 111950.

22 B. Dang, H. Chen, S. Liu, H. Liu, Z. Kang, Z. Yang, W. Yang, J. Hu and X. Chen, *Bioorg. Med. Chem. Lett.*, 2025, **127**, 130318.

23 X. Chen, J. Wang, P. Zhao, B. Dang, T. Liang, R. R. Steimbach, A. K. Miller, J. Liu, X. Wang, T. Zhang, X. Luan, J. Hu and J. Gao, *Eur. J. Med. Chem.*, 2023, **260**, 115776.

24 X. Chen, S. Zhao, H. Li, X. Wang, A. Geng, H. Cui, T. Lu, Y. Chen and Y. Zhu, *Eur. J. Med. Chem.*, 2019, **168**, 110–122.

25 X. Chen, G. Gong, X. Chen, R. Song, M. Duan, R. Qiao, Y. Jiao, J. Qi, Y. Chen and Y. Zhu, *Chem. Pharm. Bull.*, 2019, **67**, 1116–1122.

26 G. Gong, J. Qi, Y. Lv, S. Dong, C. Cao, D. Li, R. Zhao, Z. Li and X. Chen, *Chem. Pharm. Bull.*, 2020, **68**, 466–472.

27 L. Xing, G. Gong, X. Chen and X. Chen, *Chem. Pharm. Bull.*, 2023, **71**, 206–212.

28 L. Santo, T. Hideshima, A. L. Kung, J. C. Tseng, D. Tamang, M. Yang, M. Jarpe, J. H. van Duzer, R. Mazitschek,

W. C. Ogier, D. Cirstea, S. Rodig, H. Eda, T. Scullen, M. Canavese, J. Bradner, K. C. Anderson, S. S. Jones and N. Raje, *Blood*, 2012, **119**, 2579–2589.

29 P. Huang, I. Almeciga-Pinto, M. Jarpe, J. H. van Duzer, R. Mazitschek, M. Yang, S. S. Jones and S. N. Quayle, *Oncotarget*, 2017, **8**, 2694–2707.

30 A. M. Tsimberidou, P. A. Beer, C. A. Cartwright, C. Haymaker, H. H. Vo, S. Kiany, A. R. L. Cecil, J. Dow, K. Haque, F. A. Silva, L. Coe, H. Berryman, E. A. Bone, G. M. Nogueras-Gonzalez, D. Vining, H. McElwaine-Johnn and Wistuba II, *Clin. Cancer Res.*, 2021, **27**, 3584–3594.

31 T. Liang, F. Wang, R. M. Elhassan, Y. Cheng, X. Tang, W. Chen, H. Fang and X. Hou, *Acta Pharm. Sin. B*, 2023, **13**, 2425–2463.

32 V. Pathak, H. K. Maurya, S. Sharma, K. K. Srivastava and A. Gupta, *Bioorg. Med. Chem. Lett.*, 2014, **24**, 2892–2896.

33 V. Kanagarajan, J. Thanusu and M. Gopalakrishnan, *Eur. J. Med. Chem.*, 2010, **45**, 1583–1589.

34 Y. H. Lee, J. Park, S. Ahn, Y. Lee, J. Lee, S. Y. Shin, D. Koh and Y. Lim, *Daru*, 2019, **27**, 265–281.

35 C. Val, C. Rodriguez-Garcia, R. Prieto-Diaz, A. Crespo, J. Azuaje, C. Carbajales, M. Majellaro, A. Diaz-Holguin, J. M. Brea, M. I. Loza, C. Gioe-Gallo, M. Contino, A. Stefanachi, X. Garcia-Mera, J. C. Estevez, H. Gutierrez-de-Teran and E. Sotelo, *J. Med. Chem.*, 2022, **65**, 2091–2106.

36 C. A. Johnson, D. James, A. Marzan and M. Armaos, *Semin. Oncol. Nurs.*, 2019, **35**, 166–174.

37 E. M. Burd, *Clin. Microbiol. Rev.*, 2003, **16**, 1–17.

38 I. Psilopatis, N. Garmpis, A. Garmpi, K. Vrettou, P. Sarantis, E. Koustas, E. A. Antoniou, D. Dimitroulis, G. Kouraklis, M. V. Karamouzis, G. Marinos, K. Kontzoglou, A. Nonni, K. Nikolettos, F. N. Fleckenstein, C. Zoumpouli and C. Damaskos, *Cancers*, 2023, **15**, 2222.

39 X. Sun, Y. Shu, G. Ye, C. Wu, M. Xu, R. Gao, D. Huang and J. Zhang, *Acta Pharm. Sin. B*, 2022, **12**, 838–852.

40 S. Mahboobi, A. Sellmer, M. Winkler, E. Eichhorn, H. Pongratz, T. Ciossek, T. Baer, T. Maier and T. Beckers, *J. Med. Chem.*, 2010, **53**, 8546–8555.

41 O. Kinzel, L. Llauger-Bufi, G. Pescatore, M. Rowley, C. Schultz-Fademrecht, E. Monteagudo, M. Fonsi, O. Gonzalez Paz, F. Fiore, C. Steinkuhler and P. Jones, *J. Med. Chem.*, 2009, **52**, 3453–3456.

42 A. K. Oyelere, P. C. Chen, W. Guerrant, S. C. Mwakwari, R. Hood, Y. Zhang and Y. Fan, *J. Med. Chem.*, 2009, **52**, 456–468.

43 D. C. Miller, T. Reuillon, L. Molyneux, T. Blackburn, S. J. Cook, N. Edwards, J. A. Endicott, B. T. Golding, R. J. Griffin, I. Hardcastle, S. J. Harnor, A. Heptinstall, P. Lochhead, M. P. Martin, N. C. Martin, S. Myers, D. R. Newell, R. A. Noble, N. Phillips, L. Rigoreau, H. Thomas, J. A. Tucker, L. Z. Wang, M. J. Waring, A. C. Wong, S. R. Wedge, M. E. M. Noble and C. Cano, *J. Med. Chem.*, 2022, **65**, 6513–6540.